



# Non-target and suspect screening strategies for electro-dialytic soil remediation evaluation: Assessing changes in the molecular fingerprints and per- and polyfluoroalkyl substances (PFASs)

Mattias Söregård<sup>a,\*</sup>, Lutz Ahrens<sup>a</sup>, Nikiforos Alygizakis<sup>b,c</sup>, Pernille Erland Jensen<sup>d</sup>, Pablo Gago-Ferrero<sup>e,f,g,\*\*</sup>

<sup>a</sup> Swedish University of Agricultural Sciences (SLU), Department of Aquatic Sciences and Assessment, P. O. Box 7050, SE-750 07 Uppsala, Sweden

<sup>b</sup> Laboratory of Analytical Chemistry, Department of Chemistry, University of Athens, Panepistimiopolis Zografou, 15771 Athens, Greece

<sup>c</sup> Environmental Institute, Okružná 784/42, 97241 Koš, Slovak Republic

<sup>d</sup> Technical University of Denmark, Department of Civil Engineering, Brovej, 2800 Kgs. Lyngby, Denmark

<sup>e</sup> Catalan Institute for Water Research (ICRA), Carrer Emili Grahit 101, 17003 Girona, Spain

<sup>f</sup> University of Girona, Girona, Spain

<sup>g</sup> Institute of Environmental Assessment and Water Research (IDAEA-CSIC), Department of Environmental Chemistry, Jordi Girona 18-26, 08034 Barcelona, Spain

## ARTICLE INFO

Editor: GL Dotto

### Keywords:

High resolution mass spectroscopy  
Soil remediation  
Non-target screening  
Per- and polyfluoroalkyl substances  
Per fluoroheptanesulfonic acid

## ABSTRACT

Contamination of soils with organic pollutants is an increasing global problem, so novel soil remediation techniques are urgently needed. One such technique is electrokinetic remediation, in which an electric field is applied over the soil to extract contaminants. Previous evaluations of the technique have been limited to a few specific compounds. In this study, we integrated the latest advances in high-resolution mass spectrometry (HRMS) to identify molecular fingerprints, and used the results to improve the mechanistic understanding necessary for successful remediation. A laboratory-scale  $0.38 \text{ mA cm}^{-2}$  electro-dialytic treatment was applied for 21 days to a contaminated soil from a firefighter training facility in Sweden. Non-target analysis allowed generic evaluation of changes in the soil organic fraction by tentatively determining the elemental composition of compounds present. The results showed that smaller oxygen-rich molecules were significantly transported to the anode by electro-migration, while larger hydrogen-saturated molecules were transported to the cathode by electroosmotic flow. Wide suspect screening with >3000 per- and polyfluoroalkyl substances (PFASs) tentatively identified seven new PFASs in the test soil, including perfluoroheptanesulfonic acid (PFHpS), and PFASs with butoxy, ethoxy, ethanol, and ethylcyclohexanesulfonate functional groups.

## 1. Introduction

Due to unsolicited leaching of pollutants from diffuse and point sources in soil to surface water and groundwater, contaminated soils pose a risk to aquatic environments and can ultimately affect the quality of drinking water sources [1,2]. Soil remediation can reduce the risks to the environment and human health. Established and novel soil remediation technologies aim to degrade, extract, remove, or immobilize contaminants, by e.g., pump-and-treat, thermal desorption, phytoremediation, electrokinetic, and stabilization methods [3]. All remediation options have some disadvantages, such as high costs, limited applicability, a need for expert knowledge and, particularly, differing

remediation efficiency for different groups of contaminants. The latter is especially challenging as regards emerging contaminants, because it is difficult to assess the success of a specific soil remediation method owing to the high variability in physicochemical properties, and thereby behavior, of different classes of chemicals (e.g., per- and polyfluoroalkyl substances (PFASs), pesticides, pharmaceuticals, antibiotics, industrial chemicals) [4].

Recent advances in high-resolution mass spectrometry (HRMS) have opened up new opportunities for analysis of complex samples [5,6]. Additionally, new methodologies based on suspect and non-target screening [7,8] can generate knowledge that assists in selection of remediation method/s for emerging soil pollutants. Non-target and

\* Corresponding author.

\*\* Corresponding author at: Catalan Institute for Water Research (ICRA), Carrer Emili Grahit 101, 17003 Girona, Spain.

E-mail addresses: [mattias.sorengard@slu.se](mailto:mattias.sorengard@slu.se) (M. Söregård), [pgago@icra.cat](mailto:pgago@icra.cat) (P. Gago-Ferrero).

<https://doi.org/10.1016/j.jece.2020.104437>

Received 10 July 2020; Received in revised form 20 August 2020; Accepted 26 August 2020

Available online 15 September 2020

2213-3437/© 2020 The Author(s). Published by Elsevier Ltd. This is an open access article under the CC BY license (<http://creativecommons.org/licenses/by/4.0/>).

suspect screening greatly increases the number of specific substances that can be evaluated, without a prior need for standards, and enables identification of previously unknown substances [5]. Advances in non-target screening also allow evaluation of decontamination processes (e.g., water treatment) at comprehensive molecular level [9,10]. It is thereby possible to consider all molecules present in a sample without having to elucidate their structure by extensive and tedious procedures. This is an unexplored field with great possibilities to improve understanding of complex chemical remediation systems (e.g., degradation of different substances with respect to their mass or to the number of oxygen or sulfur atoms they contain) [9,10]. To our knowledge, this study is the first to apply non-target and suspect screening for soil remediation.

The fundamental concept in electrokinetic remediation of soils is to apply an electric field that extracts the pollutants from contaminated soil [11]. The electric field is generated by a power supply and is distributed by a set of electrodes inserted into the soil. Three dominant processes occur during treatment [11–14]: (i) Electromigration, i.e., transport of charged ions to opposite charge electrodes, (ii) electroosmotic flow, i.e., osmotic redistribution of water due to the change in ion concentration caused by electromigration, and (iii) electrophoresis, i.e., transportation of charged particles to electrodes of opposite charge. The direction of electromigration and electrophoresis depends on the charge on the contaminant, while electroosmotic flow is predominantly directed towards the cathode because soil is typically negatively charged and the dominant ions in soil solution are inorganic cations (e.g., magnesium ions ( $Mg^{2+}$ ) and calcium ions ( $Ca^{2+}$ )), which electromigrate to the anode. Electrokinetic remediation has been evaluated for heavy metals and organic pollutants in soil [15–17]. The remediation success is reported to be challenged by pH changes in the soil from electrode reactions due to changes in contaminant speciation, i.e., transition from ion to neutral charge or solid precipitate [18]. Unfavorable pH changes in soil can be avoided by using different means to prevent hydroxide ( $OH^-$ ) ions from entering the soil, e.g., by neutralizing titration of the electrolyte at the cathode or by separating the soil and electrolytes by ion exchange membrane (i.e., electrodialysis). Previous studies have confirmed that cationic and non-charged organic compounds are transported by electromigration and electroosmotic flow towards the cathode [19,21–23], whereas mostly negatively charged compounds such as PFASs are transported by electromigration towards the anode [17,22,24].

The overall aim of this study was to evaluate the behavior of organic compounds in electrokinetic remediation, using (i) novel non-target strategies to assess changes in molecular fingerprint and (ii) suspect screening approaches for PFASs, a known contaminant and environmentally important group [25] in the tested soil, and an emerging contaminant group of concern (considering >3000 compounds). The study took full advantage of the latest advances in HRMS and assessed a new research area for molecular fingerprinting using HRMS. The applied method used HRMS independent big data and matching algorithms based on molecular masses to transform them to possible molecular fingerprints. Changes of the molecular fingerprints were investigated for elucidation of molecular mechanisms within soil treated by the electrochemical remediation technique. In addition, to further utilize the power of HRMS, an automated suspect screening was applied to identify new pollutants of concern and their behavior in the treatment system. Both are methods that can be used for deepening our understanding of environmental and treatment processes.

## 2. Material and methods

### 2.1. Chemicals and reagents

For the electrochemical experiment sodium nitrate (VWR,  $\geq 99.5\%$  purity) and hydrochloric acid (35 %, VWR, TECHNICAL grade) was used. For the sample preparation methanol (LiChrosolv, Merck, Germany) and sodium hydroxide (VWR, Sweden) was used. For LC-HRMS

analyses, MS grade solvents (acetonitrile, methanol and HPLC water from Fisher Scientific (Germany) were used. Ammonium hydroxide 30 % PA-ACS and hydrochloric acid 37 % were supplied by Panreac (Barcelona, Spain). Formic acid 98 % was from Merck. Sodium acetate and sodium formate ( $\geq 99\%$ ) were from Sigma-Aldrich (Madrid, Spain).

### 2.2. Sampling

Composite soil samples were collected from the soil surface in a drainage channel at a firefighter training area at Stockholm Arlanda Airport, Sweden (59°39'43.005"N, 17°56'11.087"E). The site is known to be contaminated with a complex mixture of PFASs [26] due to long-term use of PFAS-containing aqueous film-forming foam (AFFF), and has been identified as a contaminant source to the aqueous environment [27]. The soil texture was found to comprise 7% sand, 34 % silt, and 59 % clay (measured by wet sieving based on a standard Swedish method (SS027123)), the soil pH was 6.0 (at a liquid:solid ratio (L/S) = 10; 691 pH Meter, Metrohm, Switzerland), the electrical conductivity was  $23 \mu S cm^{-1}$  (L/S = 10; PW 9527, Labasco Hanna instruments, USA), and the organic carbon content was 3.3 % (loss of ignition at 550 °C for 24 h).

### 2.3. Experimental set-up

A three-compartment cylindrical Plexiglas cell (diameter = 8 cm) was used to treat the soil for 21 days (Fig. 1). The outer two compartments were used for the electrodes (platinum-coated titanium rod electrodes) and electrolytes (sodium nitrate ( $NaNO_3$ ), 0.01 M, VWR,  $\geq 99.5\%$  purity) in 350 mL Millipore water, while the middle compartment (length = 10 cm) was filled with homogenized contaminated soil (1.2 kg wet weight (ww) with 22 % water content until saturation) for treatment. A fixed direct current (DC) of  $0.38 mA cm^{-2}$  was applied using 20 mA (voltage [V] ranged dynamically between 15 and 25 V) from a power supply (Hewlett Packard E3612A). The electrolytes were continuously circulated using a peristaltic pump ( $\sim 30 mL min^{-1}$ ) and, because of electrode reactions, the pH was regulated daily between 1 and 3 using hydrochloric acid (HCl, 35 %, VWR, TECHNICAL grade). The pH within the soil was regulated by preventing intrusion of protons ( $H^+$ ) and hydroxide ions ( $OH^-$ ) from the electrolytes, using a selective anion exchange membrane (SUEZ, art. No. AR204SZRA, MKIII, France) and a selective cation exchange membrane (Ionics, art. no. CR67HMP, MKIII, France), respectively.

### 2.4. Sample preparation and instrumental analysis

After 21 days of electrochemical treatment, the soil was sliced

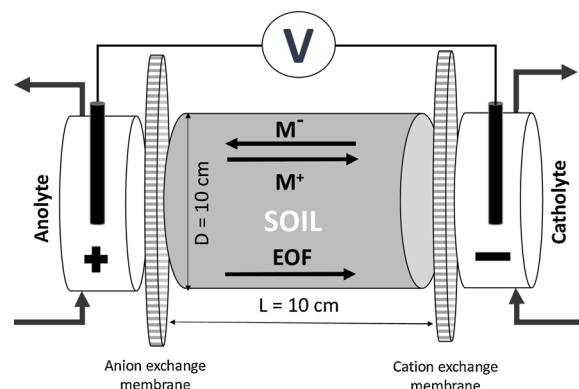


Fig. 1. Conceptual schematic of the experimental set-up of the electrochemical system, indicating the processes of electroosmotic flow (EOF), electromigration of cationic soil counter-ions ( $M^+$ ), and electromigration of anionic per- and polyfluoroalkyl substances (PFASs). Adapted from [17].

perpendicular to the electric field into 10 slices of 1.0 cm thickness and stored in darkness at 4 °C in separate sealed polypropylene (PP) bags until analysis. To properly assess the variability in the changes in molecular fingerprints and in the concentration levels of the PFASs in the samples, the sampling was conducted in triplicates, whereas untreated soil was used as reference sample. For analysis, the 10 separate slices were freeze-dried for 24 h and two-step solid-liquid extraction was performed on 3.0 g ( $n = 3$ ) dry soil, using 20 mL and then 10 mL of 80 % methanol (LiChrosolv, Merck, Germany) and 20 % 1 M laboratory-purity sodium hydroxide (VWR, Sweden) in Millipore water (Merck, Germany) solution for 1 h in an end-over-end mixer at 20 rpm. One-quarter of the combined extract was concentrated to 0.5 mL under a constant stream of nitrogen gas. The extracts were then filtered through 0.45 µm recycled cellulose syringe filters [28] into 2 mL brown glass vials (Eppendorf, Germany) and fortified with 0.5 mL of 1 M sodium hydroxide Millipore water.

Liquid chromatography (LC) coupled to HRMS analysis was performed using a LTQ-Orbitrap Velos™ coupled to the Aria TLX-1 HPLC system (Thermo Fisher Scientific, USA), in both positive and negative ionization mode. The injection volume was 10 µL and chromatographic separation was achieved using a Zorbax Eclipse XDB C18 column (150 mm x 4.6 mm, 5 µm particle size, Agilent Technologies, Santa Clara, SA). A solvent gradient with acetonitrile (A) and an aqueous solution of 10 mM formic acid/ammonium formate (pH 3) (B) was used in positive mode and a solvent gradient with acetonitrile (A) and an aqueous solution of 6.5 mM ammonium acetate/ammonia (pH = 8) (B) in negative mode. Acquisition was carried out in data-independent acquisition mode (DIA), where two sequential full scan events were triggered. The first scan was at low collision energy (4 eV) in a MS full scan over the range of  $m/z$  60–900 at a resolving power of 60,000 FWHM. The second scan was at high collision energy (35 eV) in a MS full scan over the range of  $m/z$  60–900 at a resolving power of 30,000 FWHM. The MS parameters and LC solvent gradients are listed in Section S1 and Table S1 in Supporting Information (SI).

## 2.5. Data analysis

### 2.5.1. Non-target analysis for organic compounds

Raw files acquired by LC-HRMS analysis were converted to mzML files using ProteoWizard software [29] with the following conversion parameters: *Peak Picking*, true 1-; *MSLevel*, 1–1 and *Threshold peak filter*, absolute 1000/500-most intense (positive or negative ionization mode, respectively). Peak detection was performed by the *centWave* module included in the *xcms* R-package [30], using optimized *ppm* and *peak width* parameters through Box-Behnken fractional factorial design (IPO R-package [31]). The output variable (*xcmsSet* object) was transformed to data frame in an appropriate format for import to the pattern search function of non-target R-package version 1.1.447 [32].

The elemental composition of the different compounds (i.e., MS features such as molecular ions, salt adducts, and isotopes [33]) was tentatively determined using an adapted approach described elsewhere [34]. In brief, compounds were assigned to elemental formulae ( $\text{CHON}_{0-2}\text{S}_{0-2}$ ) using an in-house formula generating R routine with the following restrictions: maximum tolerable  $m/z$  error:  $\pm 1.0$  ppm;  $m/z$  range: 100–1000; charge: only monocharged formulae were considered; range of O/C: 0–1.0; range of H/C: 0.3–2.5; range of double bond equivalent value minus the number of O atoms (DBEO): -1–10. The presence of compounds with [32]S atoms was verified by searching for the corresponding [34]S feature. Peaks, which were also detected in the blanks (HPLC water filtered and extracted with the same methodology as for the samples), were systematically removed. Although the number of compounds detected was limited by the resolution of the Orbitrap instrument, the method provided an overview of the compound composition in the soil, which helped in evaluating the behavior of organic compounds during remediation treatment.

For data evaluation, the tentatively identified compounds (and

associated variables) and their distribution over distance from the anode were evaluated with linear and polynomial (2nd order) regression and significance *t*-test tests in MATLAB, using significance level 0.05.

### 2.5.2. Suspect analysis for PFASs

For suspect screening, the NORMAN Digital Samples Freezing Platform (DSFP) was used [8]. Raw files were converted to mzML and the files generated were subjected to separation of the collision energy layers of the data-independent acquisition chromatograms in low and high collision energy mode, integrated in NORMAN DSFP. The layer-separated mzML files and their meta-data (i.e., instrumental, sample, and matrix-specific meta-data and retention time of calibrant substances (RTI)) were uploaded to the DSFP. It processed the mzML files and stored the files together with all meta-data for the generation of Data Collection Template (DCT) databases. The exact mass of the ionized form of the substances selected for screening is searched in the DCTs and only components that pass mass accuracy and fit into the expected RTI window are considered. DSFP collects all the related evidence of the identity of the substances (isotopic pattern fit, number of detected fragments, % similarity between experimental and library HRMS/MS spectra) for the detected compounds. Within the DSFP, suspect screening of 3425 PFASs (List S25 OECD PFAS LIFE APEX) was performed on the soil samples. All results were saved on the DSFP for future retrospective analysis. In addition to PFASs, the occurrence of additional 7811 contaminants with available library spectra were assessed in a similar manner with the aim to broaden the screening and make sure that no important contaminants are overlooked. The names of these substances, along with their molecular formula, SMILES, and CAS number, are provided in an Excel file in SI.

## 3. Results and discussion

### 3.1. Elucidation of molecular fingerprint

Non-target analysis was used to assess the transport behavior of the natural organic compounds in the soil. These compounds can contain a multitude of molecules with varying characteristics, including a heterogeneous mixture of polysaccharides, proteins, lipids, nucleic acids, soluble microbial products, and anthropogenic organic chemicals [35]. The mass list was generated by the *peak picking* algorithm (as described in Section 2.4.1) and, on average, over 30 000 masses [ $m/z$ ] were identified in each soil sample. Using a dissolved natural organic matter (NOM) formula-generating R routine and matching algorithm, an average of  $1140 \pm 170$  chemical formulae were assigned to each sample. No significant change in the number of NOM formulae identified was observed with distance from the anode (Fig. 2), which indicates that comparisons along the distance from the anode are valid. The relatively small variation that was observed could be explained by the effects of electro-dialytic remediation (see Section 3.2), but also variability in soil

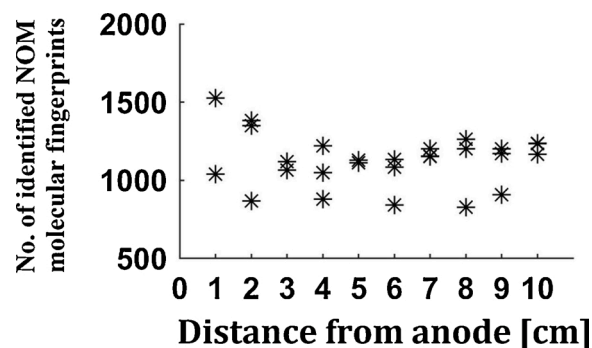


Fig. 2. Number of dissolved natural organic matter (NOM) molecular fingerprints identified as a function of distance from the anode [cm] ( $n = 3$ ) after assessing the peaks using a non-target fingerprinting strategy.

extraction conditions, as the soil closest to the anode was considerably more acidic than the rest of the soil in the sample.

Although dissolved NOM has a net negative charge [36], the organic compounds migrated to both the anode and the cathode, as indicated by the parabolic distribution of median intensity (Fig. 3A). Thus dissolved NOM can be transported by electromigration and co-transport with electroosmotic flow. This confirms previous findings that the transport vectors of organic compounds are ambivalent and impacted by electrokinetic processes and intrinsic compound properties (i.e., charge, size, etc.) [37–43]. However, the issue has not been assessed comprehensively.

### 3.2. Using molecular fingerprints to understand the electrodiolytic system

The molecular fingerprints obtained using HRMS analysis provided a fundamental understanding of the chemical processes to which organic molecules were subjected in the electrodiolytic system (Fig. 3). The results showed that the median mass was lower at the anode than at the cathode (Fig. 3A), which indicates that smaller molecules accumulated at the anode. This is in agreement with observed mean number of carbon atoms, which was on average 20 carbon atoms at the anode and 23 at the cathode (Fig. 3D). However, the change was not gradual, and no significant trend in either median mass or median number of carbon atoms was observed between 3 and 10 cm distance from the anode. Similar dependency on the number of carbon atoms and non-gradual accumulation of smaller organic micropollutants at the anode (i.e., perfluorohexanesulfonic acid (PFHxS)) has been observed previously [17]. The importance of molecular size for electrodiolytic extraction was also observed in a previous electrokinetic treatment, where the removal rate of polyaromatic hydrocarbons (PAHs) depended on molecular size and hydrophobic sorption [44]. Hydrophobic sorption is a known critical factor when predicting the environmental behavior of micropollutants and their treatment, and is related to intrinsic physicochemical properties of the micropollutants, i.e. molecular weight, solubility, and water/octanol partitioning coefficient ( $K_{OC}$ ) [4].

Although there was no gradual (linear) change in molecule size or

mean number of carbon atoms at 3–10 cm distance from the anode, there was a gradual (linear) increase in the number of hydrogen (H), nitrogen (N), and sulfur (S) atoms moving towards the cathode, as shown in Fig. 3E, G, and H, respectively. Transport of H-, N-, and S-rich molecules towards the cathode might be explained mainly by transport of larger (higher mass) organic compounds (Fig. 3A and D), which had relatively lower saturation of oxygen towards the cathode (Fig. 3F and J). Thus small oxygen-rich molecules had a higher probability of being anionically charged (e.g., with functional groups such as carboxylic acids, alcohols), and thus transported to the anode with electroosmotic flow. As a consequence, small oxygen-rich molecules had less available sites for H, N, and S (Fig. 3E, G, and H).

The abundance of oxygen-rich molecules was lower at both electrodes and highest in the middle of the soil column (Fig. 3F). This suggests that oxygen/carbon (O/C) ratio, which was significantly higher ( $p < 0.001$ ) at the anode (Fig. 3J), is a better predictor of the behavior of molecules rich in H, N, and S. Another important observation was that there was no change in average mass at 3–10 cm distance from the anode (Fig. 3A), whereas at the same time there was an increase in intensity in the 3–10 cm soil section (Fig. 3B). This could indicate that transport of organic compounds towards the cathode is concentration-dependent with relatively higher mass and relatively lower oxygen saturation.

Previous studies have shown that even compounds with net negative charge, such as oxyfluorfen (pesticide), 2,4-dichlorophenoxyacetic acid (herbicide), and phenol red (indicator dye), are transported towards the cathode due to the dominant co-transport with electroosmotic flow [24, 41]. However, some studies have found that electromigration is the dominant transport vector for compounds with net negative charge, such as chlorsulfuron (herbicide), 2,4-dichlorophenoxyacetic acid, methyl orange (indicator dye), perfluoroalkyl sulfonic acids (PFSAs), and carboxylic acids (PFCAs) [17,24,43,45]. This discrepancy in the dominant transport vector could be caused by soil characteristics, physicochemical properties of the compounds, experimental set-up, and management of the electrolyte, where an abundance of soil pore water supplied by the electrolyte increases the electroosmotic flow.

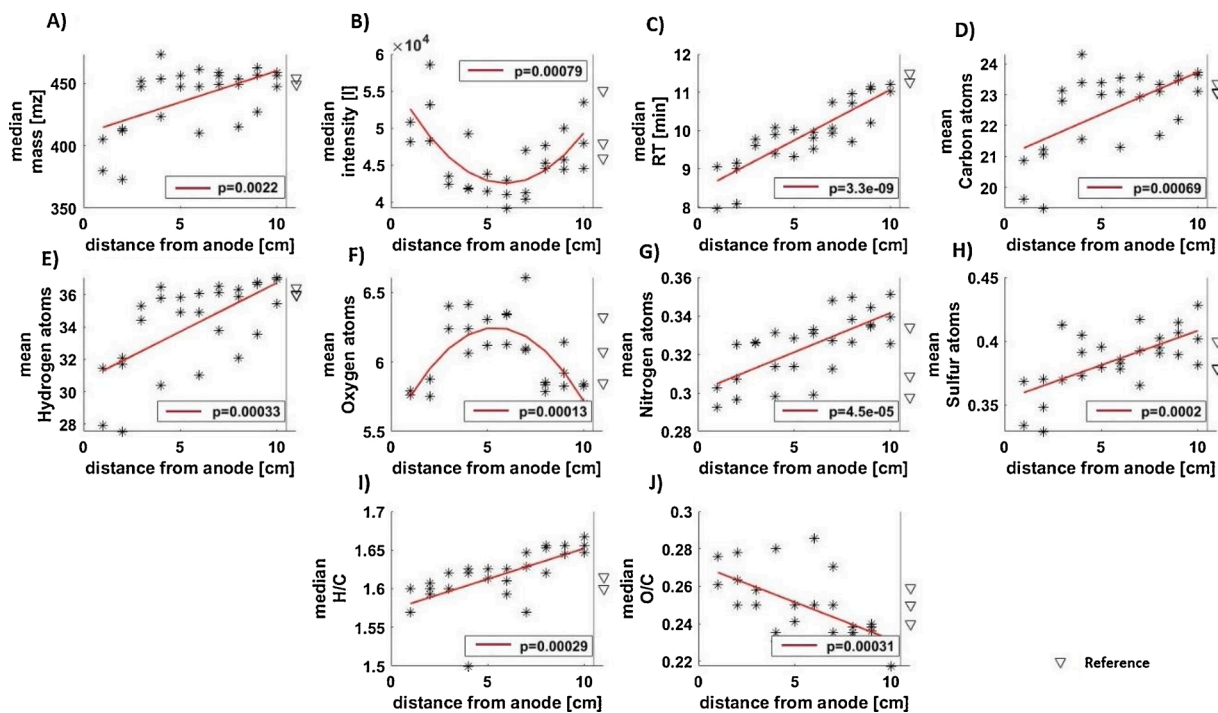


Fig. 3. (A) Median mass [ $m/z$ ], (B) median intensity [ $I$ ], (C) median retention time (RT); mean atomic composition of (D) carbon, (E) hydrogen, (F) oxygen, (G) nitrogen, and (H) sulfur; and median (I) hydrogen/carbon (H/C) ratio and (J) oxygen/carbon (O/C) ratio, based on formulae generated in a non-target fingerprint strategy, as a function of distance from the anode [cm] ( $n = 3$ ) in electrodiolytic soil remediation treatment.

Understanding the transport mechanisms is critical for designing electro-dialytic soil remediation systems, and further research is needed to determine the transport vector.

Hydrogen/carbon (H/C) ratio and O/C ratio were inversely correlated to distance from the anode (Figs. 3I and 3J, respectively). The values of H/C and O/C ratio observed indicate that the dissolved NOM composition could be categorized as lipid substances [46]. However, at the anode the average value of H/C and O/C ratio was 1.60 and 1.26, respectively, which was close to the transition from lipids towards lignin characterization of dissolved NOM [46]. In a previous study, understanding the dissolved organic fraction was shown to be an important variable for removal of heavy metals such as arsenic in an electrokinetic remediation system [47]. However, the changes in H/C and O/C ratio (Figs. 2I and 2J, respectively) were relatively small in the present study, indicating a low impact of dissolved NOM characteristics in the soil in comparison with other soil remediation methods such as landfilling [48], thermal desorption [49], and stabilization and solidification (S/S) [50]. Thus, electro-dialytic soil remediation is potentially a useful method for maintaining soil carbon, and thereby soil functioning.

Overall, this study demonstrated that molecule size, O/C ratio (including the charge on the compound), and H/C ratio were the determining factors for the transport mechanism prevailing in an electro-dialytic system. However, it was also shown from our in-depth HRMS investigation that the effect from the remediation strategy on NOM molecules were relatively small after the long 21 days of treatment.

### 3.3. Prediction of organic compound behavior in an electro-dialytic system using chromatographic retention time

The strongest correlation of the organic compounds over the soil column was with mean chromatographic retention time (RT) for each feature in the LC system ( $p < 10^{-8}$ ) (Fig. 2C). Retention time is related to the physicochemical properties of organic compounds, such as their molecule mass, charge, and/or polarity (or hydrophobicity), where compounds with lower RT (in reverse-phase chromatography) are more polar and less hydrophobic. The average RT was highest at the cathode and lowest at the anode, which is in alignment with the other results obtained in this study. Thus RT can indicate how a contaminant will behave in an electro-dialytic system. Its value can be predicted using RT




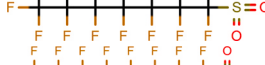
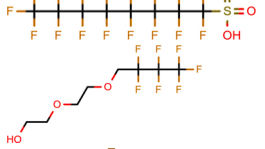
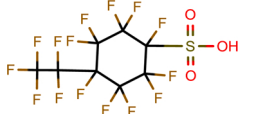
prediction models based on quantitative structure-retention relationships (QSRR), which show good performance in accurately predicting RT in a variety of chromatographic systems [51,52]. Thus RT might be a valuable tool for predicting the behavior of organic compounds in electro-dialytic soil remediation systems.

### 3.4. PFAS suspect screening

The soil treated in this study was from a PFAS-contaminated site with a known complex PFAS contamination profile [26], and therefore suspect screening was performed for 3425 individual PFASs using an approach based on the NORMAN DSFP. The confidence level in identification ranged from 3 (tentatively identified) to 1 (confirmed), based on a system described elsewhere [53]. In total, nine unique PFASs which were present in at least 50 % of the samples were tentatively identified under the criteria set for the analysis (Table 1). Three of these nine compounds (perfluorobutanesulfonic acid (PFBS), PFHxS, and perfluorooctanesulfonic acid (PFOS)) were confirmed with the corresponding analytical standard by comparison of RT and MS spectra (confidence level 1) [17]. PFBS, PFHxS, and PFOS have been detected previously in other soils at AFFF-impacted firefighter training facilities [27,54–56]. PFOS was the dominant PFAS homolog found in the present study, representing 77 % of intensity for the sum of the nine PFASs. Besides PFOS, perfluoroheptanesulfonic acid (PFHpS) was present at a high level in the soil (14 % of  $\Sigma_9$ PFASs). The presence of PFHpS is not surprising, since it is one  $\text{CF}_2$  moiety shorter than PFOS and one  $\text{CF}_2$  moiety longer than PFHxS, both of which are present in high concentrations at AFFF-contaminated sites [54,55]. However, this study showed that occurrence of PFHpS is possibly overlooked in regulations, although, based on its high intensity, it might make a considerable contribution to overall PFAS pollution. PFHpS has previously been identified in AFFFs by suspect screening [57] and quantified in drinking water with a detection frequency of 24–30 % [58,59]. Because of its close similarity to PFOS, PFHpS might have similar adverse health effects as PFOS. Thus, we recommend that the guidelines on protection of ecosystems and drinking water be updated to include PFHpS. Ultimately, the PFASs listed in Table 1 can be used as reference for future target or suspect screening studies, but it is particularly important to include PFHpS in future screening. Furthermore, perfluoroheptane

**Table 1**

Per- and polyfluoroalkyl substances (PFASs) tentatively identified by suspect screening and their molecular formula, structure, retention time [min], and level of confidence.

Name (commonly used acronym)	Molecular formula	Structure	Retention time [min]	Level of confidence <sup>a</sup>
Perfluorobutanesulfonic acid (PFBS)	$\text{C}_4\text{HF}_9\text{O}_3\text{S}$ [M-H] <sup>-</sup>		8.31	1
Perfluorohexanesulfonic acid (PFHxS)	$\text{C}_6\text{HF}_{13}\text{O}_3\text{S}$ [M-H] <sup>-</sup>		9.04	1
Perfluoroheptanesulfonic acid (PFHpS)	$\text{C}_7\text{HF}_{15}\text{O}_3\text{S}$ [M-H] <sup>-</sup>		9.48	2
Perfluorooctanesulfonic acid (PFOS)	$\text{C}_8\text{HF}_{17}\text{O}_3\text{S}$ [M-H] <sup>-</sup>		9.91	1
2-[2-(2,2,3,3,4,4,4-Heptafluorobutoxy)ethoxy]ethan-1-ol	$\text{C}_8\text{H}_{11}\text{F}_7\text{O}_3$ [M-H] <sup>-</sup>		11.36	3
Perfluoro-p-ethylcyclohexanesulfonate	$\text{C}_8\text{HF}_{15}\text{O}_3\text{S}$ [M-H] <sup>-</sup>		9.43	3

<sup>a</sup> Levels of confidence: 1 = confirmed structure, 2 = probable structure, 3 = tentative candidate.

sulfonyl fluoride (PFHpSF) and perfluorooctane sulfonyl fluoride (PFOSF) were consistently tentatively identified in soil samples ( $n = 29$  of 34 and  $n = 20$  of 34, respectively) in this study. They are the corresponding compounds to PFHpS and PFOS upon substitution of the  $-OH$  group with a fluoride ( $-F$ ), which changes the functional group to a sulfonyl fluoride. Perfluoroalkyl sulfonyl fluorides (PFSFs) are a well-known PFAS group with high production volume [60]. This group is regulated by the Stockholm Convention on persistent organic pollutants (POPs), as a precursor to PFOS [61]. However, PFSF compounds are known to be difficult to detect in LC-MS/MS systems, due to the lack of chromophores and ionizable functional groups [62,63]. PFHpSF and PFOSF released into the environment has been shown to ultimately be transformed to PFHpS and PFOS [64]. The identifications of PFOSF and PFHpSF were discarded after purchasing and injecting analytical standards. A careful inspection of the chromatograms showed that the suspected peaks of PFOSF and PFHpSF corresponded to isotopic peaks of PFOS and PFHpS, respectively, with very similar masses and same retention time. Thus, these compounds were removed from list of tentatively identified new PFASs. This case shows the requirement of expertise knowledge when utilizing automated suspect screening methodologies based on HRMS.

Two additional PFASs, 2-[2-(2,2,3,3,4,4,4-heptafluorobutoxy)ethoxy]ethan-1-ol and perfluoro-*p*-ethylcyclohexanesulfonate, were tentatively identified (level 3, tentative candidates). To the best of our knowledge, these compounds have not been detected previously in extensive PFAS target studies [65] or in suspect screening studies [66, 67], and should be considered in further analyses.

PFOS showed a significant linear correlation with distance [cm] from the anode ( $R^2 = 0.72$ ,  $p < 0.01$ ; Fig. 4A), whereas no significant correlation was found for PFHpS ( $R^2 = 0.23$ ,  $p = 0.074$ ; Fig. 4B). The peak intensity of PFOS in this study was significantly linearly correlated to target analysis from a previous study [17] using the same experimental set-up ( $R^2 = 0.69$ ,  $p < 0.01$ ) (Figure S2 in SI). The other tentatively identified PFASs did not show significant spatial distribution trends over distance [cm] from the anode, which might be due to the low peak intensity and thus high relative standard deviation preventing identification of spatial trends. Overall, the suspect screening in this study did not generate enough data to provide a general understanding of the molecular behavior of the tentatively identified PFASs in an electrokinetic remediation system. However, the results enabled a better understanding of the contamination profile in the study soil. The methodology could easily be transferred to other remediation systems dealing with a highly concentrated and complex mixture of pollutants. Apart from PFASs, eight additional substances (mainly surfactants) were consistently tentatively identified in the soil samples. The identity of these substances, identification details, and behavior during the process are explained in detail in SI.

#### 4. Conclusions

High-resolution mass spectrometry improved understanding of electrokinetic soil remediation at an in-depth level that would not have been possible otherwise. By analyzing changes in the molecular fingerprint of  $>1000$  dissolved NOM compounds in contaminated soil, we observed that relatively smaller and oxygen-rich molecules (probably with net anionic charge) were subjected to electromigration towards the anode, while more hydrophobic compounds were transported with electroosmotic flow towards the cathode. This shows the importance of the physicochemical properties of organic chemicals for the removal process. Retention time in liquid chromatography, which depended on the molecular mass, charge, and polarity of the molecules identified, was a strong predictor for the transport behavior of molecules in the electrokinetic system. Thus, RT prediction models can be used in future for predicting the transport behavior of organic compounds in electrokinetic soil treatments. Non-target screening was useful for determining trends and the fundamentals of the soil remediation treatment, and can

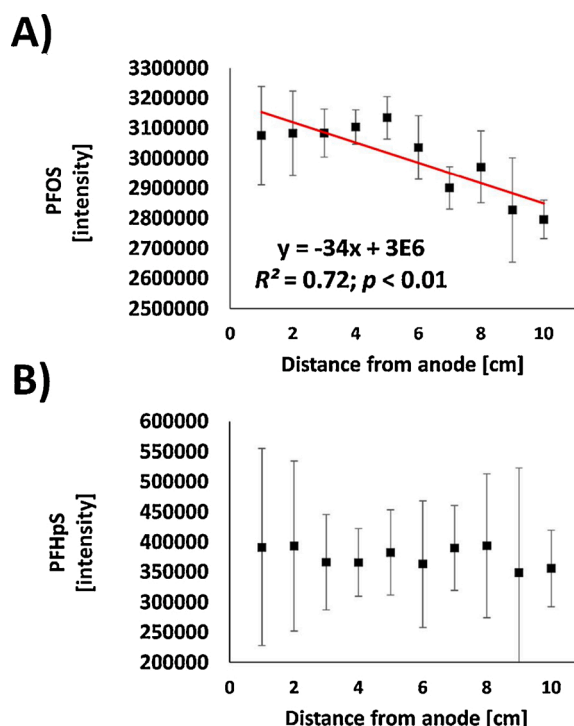


Fig. 4. Intensity of two tentatively identified per- and polyfluoroalkyl substances (PFASs) over the distance from the anode [cm] in the electrokinetic soil remediation treatment. (A) Perfluorooctanesulfonic acid (PFOS) and (B) perfluoroheptanesulfonic acid (PFHpS).

be a valuable tool in development and optimization of future treatment techniques. Use of a suspect screening approach allowed tentative identification of seven additional PFASs, three of which were confirmed (PFBS, PFHxS, and PFOS). PFOS and PFHpS were ubiquitously present in the soil at high intensity, but have been overlooked (particularly PFHpS) in previous studies. Overall, the method followed was largely automated, and can easily be applied for non-target screening of molecular fingerprints and suspect screening strategies in other environmental remediation systems.

#### CRediT authorship contribution statement

**Mattias Söregård:** Conceptualization, Methodology, Software, Investigation, Writing - original draft, Visualization. **Lutz Ahrens:** Supervision, Writing - review & editing, Funding acquisition. **Nikiforos Alygizakis:** Software, Writing - review & editing. **Pernille Erland Jensen:** Methodology, Supervision, Writing - review & editing. **Pablo Gago-Ferrero:** Conceptualization, Methodology, Writing - original draft, Supervision, Funding acquisition.

#### Declaration of Competing Interest

The authors report no declarations of interest.

#### Acknowledgements

This work was supported by the project PFAS-PURE from VINNOVA, Sweden (2015-03561). Pablo Gago-Ferrero acknowledges the European Union's Horizon 2020 research and innovation program under the Marie Skłodowska-Curie grant agreement Smart-Workflow No 747698. The authors acknowledge the Trace Analysis and Mass Spectrometry Group (TrAMS of the University of Athens) for support with chemometric tools, and the Danish Technical University (DTU BYG) for experimental support.

## Appendix A. Supplementary data

Supplementary material related to this article can be found, in the online version, at doi:<https://doi.org/10.1016/j.jece.2020.104437>.

## References

- [1] M. Murakami, et al., Groundwater pollution by perfluorinated surfactants in Tokyo, *Environ. Sci. Technol.* 43 (2009) 3480–3486.
- [2] Y. Li, D.P. Oliver, R.S. Kookana, A critical analysis of published data to discern the role of soil and sediment properties in determining sorption of per and polyfluoroalkyl substances (PFASs), *Sci. Total Environ.* 628–629 (2018) 110–120.
- [3] *Soil Pollution - Origin, Monitoring & Remediation* | Ibrahim Mirsal | Springer. (2017).
- [4] A. Rostvall, et al., Removal of pharmaceuticals, perfluoroalkyl substances and other micropollutants from wastewater using lignite, Xylit, sand, granular activated carbon (GAC) and GAC+Polonite® in column tests – role of physicochemical properties, *Water Res.* 137 (2018) 97–106.
- [5] P. Gago-Ferrero, et al., Extended suspect and non-target strategies to characterize emerging polar organic contaminants in raw wastewater with LC-HRMS/MS, *Environ. Sci. Technol.* 49 (2015) 12333–12341.
- [6] J. Hollender, E.L. Schymanski, H.P. Singer, P.L. Ferguson, Nontarget screening with high resolution mass spectrometry in the environment: ready to go? *Environ. Sci. Technol.* 51 (2017) 11505–11512.
- [7] N.A. Alygizakis, P. Gago-Ferrero, J. Hollender, N.S. Thomaidis, Untargeted time-pattern analysis of LC-HRMS data to detect spills and compounds with high fluctuation in influent wastewater, *J. Hazard. Mater.* 361 (2019) 19–29.
- [8] N.A. Alygizakis, et al., NORMAN digital sample freezing platform: a European virtual platform to exchange liquid chromatography high resolution-mass spectrometry data and screen suspects in “digitally frozen” environmental samples, *TrAC Trends Anal. Chem.* 115 (2019) 129–137.
- [9] Y. Verkh, M. Rozman, M. Petrovic, A non-targeted high-resolution mass spectrometry data analysis of dissolved organic matter in wastewater treatment, *Chemosphere* 200 (2018) 397–404.
- [10] G. Nürenberg, et al., Nontarget analysis: a new tool for the evaluation of wastewater processes, *Water Res.* 163 (2019) 114842.
- [11] Y.B. Acar, A.N. Alshawabkeh, Principles of electrokinetic remediation, *Environ. Sci. Technol.* 27 (1993) 2638–2647.
- [12] J. Virkutyte, M. Sillanpää, P. Latostenmaa, Electrokinetic soil remediation – critical overview, *Sci. Total Environ.* 289 (2002) 97–121.
- [13] A.B. Ribeiro, J.M. Rodríguez-Maroto, E.P. Mateus, H. Gomes, Removal of organic contaminants from soils by an electrokinetic process: the case of atrazine. Experimental and modeling, *Chemosphere* 59 (2005) 1229–1239.
- [14] R.T. Gill, M.J. Harbottle, J.W.N. Smith, S.F. Thornton, Electrokinetic-enhanced bioremediation of organic contaminants: a review of processes and environmental applications, *Chemosphere* 107 (2014) 31–42.
- [15] J.-H. Chang, Y.-L. Wang, S.-Y.A. Shen, Specific configuration of circulation-enhanced electrokinetics (CEEK) to remediate real-site Cd and Pb contaminated soils, *J. Hazard. Mater.* 359 (2018) 408–413.
- [16] I.C. Paixão, et al., Electrokinetic-Fenton for the remediation low hydraulic conductivity soil contaminated with petroleum, *Chemosphere* 248 (2020).
- [17] M. Sörensgrård, G. Niarchos, P.E. Jensen, L. Ahrens, Electrolytic per- and polyfluoroalkyl substances (PFASs) removal mechanism for contaminated soil, *Chemosphere* 232 (2019) 224–231.
- [18] H.K. Hansen, et al., Electrolytic remediation of soil polluted with heavy metals. Key parameters for optimization of the process, *Chem. Eng. Res. Des.* 77 (1999) 218–222.
- [19] A.B. Ribeiro, E.P. Mateus, J.-M. Rodríguez-Maroto, Removal of organic contaminants from soils by an electrokinetic process: the case of molinate and bentazone. Experimental and modeling, *Sep. Purif. Technol.* 79 (2011) 193–203.
- [20] P. Guedes, et al., Electrolytic treatment of sewage sludge: current intensity influence on phosphorus recovery and organic contaminants removal, *Chem. Eng. J.* 306 (2016) 1058–1066.
- [21] F.L. Souza, C. Sáez, M.R.V. Lanza, P. Cañizares, M.A. Rodrigo, Removal of chloresulfuron and 2,4-D from spiked soil using reversible electrokinetic adsorption barriers, *Sep. Purif. Technol.* 178 (2017) 147–153.
- [22] L.M. Ottsen, et al., Electrokinetics applied in remediation of subsurface soil contaminated with chlorinated ethenes – a review, *Chemosphere* 235 (2019) 113–125.
- [23] E.M. Yusni, S. Tanaka, Removal behaviour of a thiazine, an azo and a triarylmethane dyes from polluted kaolinitic soil using electrokinetic remediation technology, *Electrochim. Acta* 181 (2015) 130–138.
- [24] L. Ahrens, Polyfluoroalkyl compounds in the aquatic environment: a review of their occurrence and fate, *J. Environ. Monit.* 13 (2011) 20–31.
- [25] L. Gobelius, J. Lewis, L. Ahrens, Plant uptake of per- and polyfluoroalkyl substances at a contaminated fire training facility to evaluate the phytoremediation potential of various plant species, *Environ. Sci. Technol.* 51 (2017) 12602–12610.
- [26] L. Ahrens, K. Norström, T. Viktor, A.P. Cousins, S. Josefsson, Stockholm Arlanda Airport as a source of per- and polyfluoroalkyl substances to water, sediment and fish, *Chemosphere* 129 (2015) 33–38.
- [27] M. Sörensgrård, V. Franke, R. Tröger, L. Ahrens, Losses of poly- and perfluoroalkyl substances to syringe filter materials, *J. Chromatogr. A* 1609 (2020).
- [28] M.C. Chambers, et al., A cross-platform toolkit for mass spectrometry and proteomics, *Nat. Biotechnol.* 30 (2012) 918–920.
- [29] R. Tautenhahn, C. Böttcher, S. Neumann, Highly sensitive feature detection for high resolution LC/MS, *BMC Bioinformatics* 9 (2008) 504.
- [30] G. Libiseller, et al., IPO: a tool for automated optimization of XCMS parameters, *BMC Bioinformatics* 16 (2015) 118.
- [31] M. Loos, Nontarget: Detecting Isotope, Adduct and Homologue Relations in LC-MS Data, 2020.
- [32] P.A. Lara-Martín, A.C. Chiaia-Hernández, M. Biel-Maeso, R.M. Baena-Nogueras, J. Hollender, Tracing urban wastewater contaminants into the Atlantic ocean by nontarget screening, *Environ. Sci. Technol.* (2020), <https://doi.org/10.1021/acs.est.9b06114>.
- [33] M.J. Farré, A. Jaén-Gil, J. Hawkes, M. Petrovic, N. Catalán, Orbitrap molecular fingerprint of dissolved organic matter in natural waters and its relationship with NDMA formation potential, *Sci. Total Environ.* 670 (2019) 1019–1027.
- [34] A. Nebbioso, A. Piccolo, Molecular characterization of dissolved organic matter (DOM): a critical review, *Anal. Bioanal. Chem.* 405 (2013) 109–124.
- [35] D.G. Kinniburgh, et al., Ion binding to natural organic matter: competition, heterogeneity, stoichiometry and thermodynamic consistency, *Colloids Surf. Physicochem. Eng. Asp.* 151 (1999) 147–166.
- [36] H.I. Chung, M. Lee, A new method for remedial treatment of contaminated clayey soils by electrokinetics coupled with permeable reactive barriers, *Electrochim. Acta* 52 (2007) 3427–3431.
- [37] M. Gholami, D.Y. Kebria, M. Mahmudi, Electrokinetic remediation of perchloroethylene-contaminated soil, *Int. J. Environ. Sci. Technol. (Tehran)* 11 (2014) 1433–1438.
- [38] P. Guedes, E.P. Mateus, N. Couto, Y. Rodríguez, A.B. Ribeiro, Electrokinetic remediation of six emerging organic contaminants from soil, *Chemosphere* 117 (2014) 124–131.
- [39] J.-Y. Lee, et al., Electrokinetic (EK) removal of soil co-contaminated with petroleum oils and heavy metals in three-dimensional (3D) small-scale reactor, *Process Saf. Environ. Prot.* 99 (2016) 186–193.
- [40] R. López-Vizcaino, et al., Scale-up of the electrokinetic fence technology for the removal of pesticides. Part I: some notes about the transport of inorganic species, *Chemosphere* 166 (2017) 540–548.
- [41] C. Ruiz, E. Mena, P. Cañizares, J. Villaseñor, M.A. Rodrigo, Removal of 2,4,6-Trichlorophenol from Spiked Clay Soils by Electrokinetic Soil Flushing Assisted with Granular Activated Carbon Permeable Reactive Barrier, *Ind. Eng. Chem. Res.* 53 (2014) 840–846.
- [42] F.L. Souza, C. Sáez, M.R.V. Lanza, P. Cañizares, M.A. Rodrigo, Removal of chloresulfuron and 2,4-D from spiked soil using reversible electrokinetic adsorption barriers, *Sep. Purif. Technol.* 178 (2017) 147–153.
- [43] M.T. Alcántara, J. Gómez, M. Pazos, M.A. Sanromán, Electrokinetic remediation of PAH mixtures from kaolin, *J. Hazard. Mater.* 179 (2010) 1156–1160.
- [44] C. Risco, et al., Remediation of soils polluted with 2,4-D by electrokinetic soil flushing with facing rows of electrodes: A case study in a pilot plant, *Chem. Eng. J.* 285 (2016) 128–136.
- [45] A.C. Maizel, C.K. Remucal, The effect of advanced secondary municipal wastewater treatment on the molecular composition of dissolved organic matter, *Water Res.* 122 (2017) 42–52.
- [46] J. Li, et al., Comparison of humic and fulvic acid on remediation of arsenic contaminated soil by electrokinetic technology, *Chemosphere* 241 (2020).
- [47] L. Ahrens, et al., Wastewater treatment plant and landfills as sources of polyfluoroalkyl compounds to the atmosphere, *Environ. Sci. Technol.* 45 (2011) 8098–8105.
- [48] E. Crownover, D. Oberle, M. Kluger, G. Heron, Perfluoroalkyl and polyfluoroalkyl substances thermal desorption evaluation, *Remediat. J.* 29 (2019) 77–81.
- [49] M. Sörensgrård, D.B. Kleja, L. Ahrens, Stabilization and solidification remediation of soil contaminated with poly- and perfluoroalkyl substances (PFASs), *J. Hazard. Mater.* 367 (2019) 639–646.
- [50] R. Aalizadeh, N.S. Thomaidis, A.A. Bletsou, P. Gago-Ferrero, Quantitative structure–Retention relationship models to support nontarget high-resolution mass spectrometric screening of emerging contaminants in environmental samples, *J. Chem. Inf. Model.* 56 (2016) 1384–1398.
- [51] R. Aalizadeh, M.-C. Nika, N.S. Thomaidis, Development and application of retention time prediction models in the suspect and non-target screening of emerging contaminants, *J. Hazard. Mater.* 363 (2019) 277–285.
- [52] E.L. Schymanski, et al., Identifying small molecules via high resolution mass spectrometry: communicating confidence, *Environ. Sci. Technol.* 48 (2014) 2097–2098.
- [53] C. Baduel, C.J. Paxman, J.F. Mueller, Perfluoroalkyl substances in a firefighting training ground (FTG), distribution and potential future release, *J. Hazard. Mater.* 296 (2015) 46–53.
- [54] M. Filipovic, et al., Historical usage of aqueous film forming foam: a case study of the widespread distribution of perfluoroalkyl acids from a military airport to groundwater, lakes, soils and fish, *Chemosphere* 129 (2015) 39–45.
- [55] J. Bräunig, et al., Fate and redistribution of perfluoroalkyl acids through AFFF-impacted groundwater, *Sci. Total Environ.* 596–597 (2017) 360–368.
- [56] A. Rotander, et al., Novel fluorinated surfactants tentatively identified in firefighters using liquid chromatography quadrupole time-of-flight tandem mass spectrometry and a case-control approach, *Environ. Sci. Technol.* 49 (2015) 2434–2442.
- [57] R. Loos, et al., Pan-European survey on the occurrence of selected polar organic persistent pollutants in ground water, *Water Res.* 44 (2010) 4115–4126.
- [58] H.A. Kaboré, et al., Worldwide drinking water occurrence and levels of newly-identified perfluoroalkyl and polyfluoroalkyl substances, *Sci. Total Environ.* 616–617 (2018) 1089–1100.

- [60] A.G. Paul, K.C. Jones, A.J. Sweetman, A First Global Production, Emission, And Environmental Inventory For Perfluorooctane Sulfonate, *Environ. Sci. Technol.* 43 (2009) 386–392.
- [61] G.W. Olsen, J.M. Burris, J.H. Mandel, L.R. Zobel, Serum perfluorooctane sulfonate and hepatic and lipid clinical chemistry tests in fluorochemical production employees, *J. Occup. Environ. Med.* 41 (1999) 799–806.
- [62] C. Sun, H. Sun, Y. Lai, J. Zhang, Z. Cai, Liquid Chromatography/Mass spectrometry method for determination of perfluorooctane sulfonyl fluoride upon derivatization with benzylamine, *Anal. Chem.* 83 (2011) 5822–5826.
- [63] X. Li, X. Wang, T. Fang, L. Zhang, J. Gong, Disposable photoelectrochemical sensing strip for highly sensitive determination of perfluorooctane sulfonyl fluoride on functionalized screen-printed carbon electrode, *Talanta* 181 (2018) 147–153.
- [64] Z. Wang, J.M. Boucher, M. Scheringer, I.T. Cousins, K. Hungerbühler, Toward a comprehensive global emission inventory of C4–C10 perfluoroalkanesulfonic acids (PFASs) and related precursors: focus on the life cycle of C8-Based products and ongoing industrial transition, *Environ. Sci. Technol.* 51 (2017) 4482–4493.
- [65] G. Munoz, et al., Optimization of extraction methods for comprehensive profiling of perfluoroalkyl and polyfluoroalkyl substances in firefighting foam impacted soils, *Anal. Chim. Acta* 1034 (2018) 74–84.
- [66] K.A. Barzen-Hanson, et al., Discovery of 40 classes of per- and polyfluoroalkyl substances in historical aqueous film-forming foams (AFFFs) and AFFF-Impacted groundwater, *Environ. Sci. Technol.* 51 (2017) 2047–2057.
- [67] Y. Liu, L.A. D'Agostino, G. Qu, G. Jiang, J.W. Martin, High-resolution mass spectrometry (HRMS) methods for nontarget discovery and characterization of poly- and per-fluoroalkyl substances (PFASs) in environmental and human samples, *TrAC Trends Anal. Chem.* 121 (2019) 115420.